

Photophysical, Electrochemical, and Theoretical Study of Protriptyline in Several Solvents

Carmelo García,^{*,†} Rolando Oyola,[‡] Luis Piñero,[†] Nadya Cruz,[†] Felix Alejandro,[‡] Rafael Arce,[‡] and Ileana Nieves[†]

Department of Chemistry, University of Puerto Rico, Humacao Campus, 100 Road 908, Humacao, Puerto Rico 00791-4300, and University of Puerto Rico, Río Piedras Campus, P.O. Box 23346, Río Piedras, Puerto Rico 00931-3346

Received: April 18, 2002; In Final Form: June 4, 2002

Photophysical and electrochemical properties of protriptyline hydrochloride (PTL-HCl) and its free base were measured in different solvents. Ground-state properties remain unchanged as a function of solvent or protonation state. The fluorescence quantum yield and lifetime, on the other hand, are solvent-dependent. Fluorescence lifetimes results were obtained from monoexponential decay fittings. Characterization of the 266 nm nanosecond laser flash photolysis species reveals the presence of the triplet–triplet transient intermediate at low-intensity conditions. At high laser intensities, two new transient intermediates were observed, which were assigned to the solvated electron and the radical cation. These species are formed through a biphotonic route, as shown with photonicity studies. The relatively high oxidation potentials measured for PTL-HCl and its free base corroborate the biphotonic process required for these species. These electrochemical studies also show that PTL-HCl is easier to oxidize than its free base. Singlet oxygen is established as one of the transient species following triplet-state formation. The PTL-HCl triplet state is probably involved in the dimer formation and other reactive intermediates, and therefore, it might be directly associated with the *in vivo* phototoxic effects observed for this drug.

Introduction

The mechanisms of the cutaneous photosensitivity of many drugs are still unknown. Protriptyline hydrochloride (PTL-HCl), a tricyclic antidepressant (TCA), is a skin photosensitizing agent in humans.¹ It has been proposed that PTL-HCl acts by both photodynamic and nonphotodynamic processes.² PTL-HCl photosensitizes red blood cell lysis, suggesting that cell membranes may be the sites of light-induced damage.³ Kochevar and Gasparro investigated the photochemical behavior of PTL-HCl under anaerobic and aerobic conditions and found that it photodecomposes producing a complex mixture of products.² Preirradiated PTL-HCl also caused red blood cell lysis *in vitro* and erythema in guinea pigs when injected intradermally. Under anaerobic conditions, some of the detected photoproducts are responsible for the red blood cell lysis. One of these was identified as the cyclobutyl dimer of PTL-HCl.² The mechanisms postulated for the formation of this product involve the participation of the PTL-HCl triplet state, although it was not identified. These authors also reported the fluorescence quantum yield, ϕ_f , of PTL-HCl in different solvents. The ϕ_f of PTL-HCl varied with solvent polarity and basicity. In aqueous solution (pH = 5.1) and ethanol, a ϕ_f of 0.81 was reported, but in DMSO, the yield was only 0.30. These differences were explained in terms of different equilibria of PTL-HCl in solution, in which the existing species also depend on the solvent. These species include the PTL-HCl cation, dimers, the solvated PTL free base, and the PTL-HCl solvated pair. Low ϕ_f values correspond to solvents in which the free amino group can quench the PTL-HCl fluorescence. However, high ϕ_f values in aqueous solutions implicate a low triplet yield. These results show that there is a

direct relationship between the PTL-HCl photophysical properties and its phototoxicity.

Photoirradiation of PTL-HCl under oxygen allowed Sharples and Jones to characterize the main PTL-HCl photoproducts.⁴ Among those were the 10-hydroxyprotriptyline and the protriptyline 10,11-epoxide, which subsequently transformed to the 10,11-dihydroxyprotriptyline diol. The triplet state was proposed as precursor for these products, producing either singlet oxygen or superoxide intermediates through energy- or charge-transfer processes.

Until now, there are no reports on the identification and properties of the reactive intermediates participating in the photodynamic response and nonphotodynamic processes of PTL-HCl. However, there are several reports on the photophysical properties of the PTL parent compound, 5*H*-dibenzo[*a,d*]cycloheptene (DBCH), and some other derivatives.^{5–10} Although the biological activities of PTL-HCl and DBCH are different, the interest in the latter is due to its relevance as a reaction intermediate in organic synthesis or as a model for the *cis*–*trans* stilbene photophysical properties. The biological activity of PTL-HCl is attributed to the presence of the methylpropylamine side chain at C₅ (Figure 1).

We report here the results of the absorption, emission, laser flash photolysis, and electrochemical studies of PTL-HCl and its free base. It is well-known that this type of compound is hydrophobic and has high affinity for nonpolar membranes. In this environment, the nonprotonated form has the higher contribution and should determine the photophysics of the system. Quantum chemical calculations were performed to properly assign the contributions of each atomic orbital to the corresponding electronic transitions. This information is important to establish whether any changes in the photophysical properties of DBCH are actually introduced by the alkyl chain. Finally, the quantum yield of singlet oxygen formation was

* To whom correspondence should be addressed. Phone: (787) 850-9387. Fax: (787) 850-9422. E-mail: C_Garcia@cuhac.upr.clu.edu.

[†] University of Puerto Rico, Humacao Campus.

[‡] University of Puerto Rico, Río Piedras Campus.

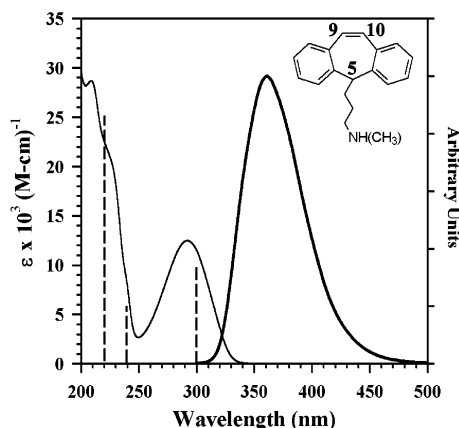


Figure 1. PTL-HCl ground-state molar absorption spectrum with vertical lines indicating the calculated oscillator strengths (left) and emission spectrum (right) in PBS 7.4. The inset shows the PTL molecular structure.

determined, and its participation in the above outlined photochemistry is discussed.

Experimental Section

Protriptyline hydrochloride, benzophenone (BP), phenalene (PH), *p*-nitrosodimethylaniline (RNO), NaN_3 , and naphthalene (NP) were purchased from Sigma-Aldrich Chemical Co. (St. Louis, MO). Tetrabutylammonium perchlorate (TBAP) was purchased from GFS Chemicals (Columbus, OH) and was recrystallized from ethyl acetate. High-quality-grade organic solvents were acquired from well-known suppliers. Nitrogen and nitrous oxide were purchased from Air Products (Humacao, PR). Aqueous solutions were prepared with nanopure water. The protriptyline free base (PTL) was obtained by adding an excess of NaOH to a PTL-HCl aqueous solution followed by ether extraction.

Absorption and Emission Spectroscopy. Absorption spectra were taken with a HP 8453 UV-vis photodiode array spectrophotometer. Luminescence was measured with a Spex Fluorolog Tau 3.11 spectrofluorimeter with fluorescence lifetimes capabilities (Spex Industries, NJ). The fluorescence quantum yield (ϕ_f) was obtained relative to tryptophan ($\phi_f = 0.13$)¹¹ according to Demas and Crosby.¹² The excitation wavelength was 280 nm, reference and samples were optically matched ($\text{OD} < 0.1$), and the monochromator slits were both set at 2.0 nm. Corrections were made for differences in the instrument sensitivity as a function of wavelength and for differences in refractive index. Frequency-dependent emissions were obtained against a scatter solution for the determination of the fluorescence lifetime.¹¹ Lifetime regression analysis was performed with the software developed by the Center for Fluorescence Spectroscopy (Baltimore, MD).

Laser Flash Spectroscopy. Transient intermediates were generated with the third (355 nm) or fourth (266 nm) harmonic output of a Continuum Surelite II (Santa Clara, CA). The laser energy was measured with an energy/power meter from Newport, model 1835, coupled to a detector, model 818J-50. Transient species were monitored at right angles to the unfocused laser beam using a 300 W xenon arc lamp (Oriental Corp.). The probe beam was discriminated with a monochromator model 301 (Acton Research) and detected with a Hamamatsu R928 five-stage dynode-wired photomultiplier tube.¹³ Output from the photomultiplier was digitized with a 400 MHz bandwidth oscilloscope, model 9310 (Lecroy Corp.), and transferred to the computer through GPIB communication

for analysis. A flow system was used to ensure a fresh sample for each laser pulse. All of the spectrokinetic system was controlled with an in-house-developed Labview 5.1-based application software (National Instruments, Austin, TX). Kinetic decays analysis was carried out using Levenberg-Marquardt nonlinear fitting programs under Labview 5.1.

Determination of Triplet Absorption Coefficient (ϵ_T). Triplet absorption coefficients were measured in solution using the energy-transfer method.¹⁴ Briefly, a solution of benzophenone (BP) in CH_3CN was excited at 355 nm in the absence and in the presence of a 0.8 mM solution of the drug. Under these conditions, all laser light was absorbed by BP. From the transient absorbencies of the BP triplet in the absence of the PTL derivative and of the sensitized drug triplet following energy transfer from the BP donor and by using $\epsilon_T = 6500 \text{ M}^{-1} \text{ cm}^{-1}$ for BP at 520 nm,¹⁴ we determined the unknown ϵ_T values according to the following equation:

$$\epsilon_T^X = \left(\frac{\Delta \text{OD}_T^X}{\Delta \text{OD}_T^{\text{BP}}} \right) \epsilon_T^{\text{BP}} \quad (1)$$

Kinetic corrections were applied for less than 100% energy transfer.¹⁴ The maximum error for the reported ϵ values is approximately 12% of the measured value.

Quantum Yields of Triplet Formation (ϕ_T). This value was obtained by the comparative actinometry method using naphthalene (NP) in cyclohexane as reference ($\phi_T = 0.75$, $\epsilon_T = 24\,500 \text{ M}^{-1} \text{ cm}^{-1}$ at 414 nm).¹⁴ Optically matched samples of NP and the drug were irradiated at 266 nm in different nitrogen-saturated solvents. The triplet-state absorbance of NP and the drug at 414 and 420 nm, respectively, were measured at low laser energy ($E < 5 \text{ mJ}$). Triplet transient ODs were then used to calculate ϕ_T for PTL-HCl and PTL according to the following equation:

$$\phi_T^X = \left(\frac{\text{OD}_T^X \epsilon_T^{\text{NP}}}{\text{OD}_T^{\text{NP}} \epsilon_T^X} \right) \phi_T^{\text{NP}} \quad (2)$$

Quantum Yield of $^1\text{O}_2$ Formation. This value was determined from the reaction of singlet oxygen with imidazole, followed by the reaction of its trans-annular peroxide product with *p*-nitrosodimethylaniline (RNO).¹⁵ Consumption of RNO was measured at 440 nm ($\epsilon = 34\,200 \text{ M}^{-1} \text{ cm}^{-1}$)¹⁶ as a function of time during the 313 nm irradiation of air-saturated PTL-HCl and phenalene (PH) samples. The quantum yield for singlet oxygen formation was obtained using eq 3, where S is the slope obtained from the plot of $A_{440\text{nm}}$ against time and X and R refers to unknown and reference compound, respectively.¹⁷

$$\phi_{^1\text{O}_2}^X = \left(\frac{S_X}{S_R} \right) \phi_{^1\text{O}_2}^R \quad (3)$$

Electrochemical Measurements. Electrochemical experiments were performed with a voltammetric analyzer, BAS model CV-50W. Solutions of PTL-HCl or PTL (3.0 mM) in acetonitrile or methanol containing 0.1 M tetrabutylammonium perchlorate as supporting electrolyte were degassed with nitrogen before use. The measurements were carried out using a glassy carbon as working electrode, a platinum wire as counter electrode, and Ag/AgCl(sat) ($E^0 = +0.222 \text{ V}$) as reference electrode. It is not possible to obtain oxidation potentials in aqueous solutions due to the limitation in the available oxidation range for this solvent under our experimental conditions ($-1.5 \leq V \leq 1.5$).

PM3/CI Theoretical Calculations. Geometry optimization using a combination of molecular mechanics (MM+), molecular dynamics, and quantum mechanical calculations for closed shells (PM3/RHF/CI) and open shells (PM3/UHF) were performed with HyperChem 6.03 (HyperCube Inc., FL) running on an SGI-320 with dual 450 MHz processors (Silicon Graphics, CA). MM+ was used to preoptimize all closed-shell systems. At the semiempirical level, the optimizations were done with the Polak–Ribiere conjugated gradient protocol (1×10^{-5} convergence limit, 0.001 kcal/(Å mol) rms limit). The lowest-energy conformations were found by randomly varying the chain dihedral angle. To make sure that the counterion remains at the standard distance in the PTL-HCl system, the $H^+ \cdots Cl^-$ separation was restrained to 1.32 Å with the default force constant (7 kcal/(mol Å)). All molecular parameters were obtained with PM3/RHF/CI single-point calculations starting with the most stable PM3-optimized conformation and using three occupied and three virtual orbitals. The triplet energy is obtained from the difference between the formation enthalpy of the T_1 and the S_0 states. The gas-phase ionization potential (IP_g) was either taken as the negative of the HOMO energy (Koopman's theorem) or calculated from the formation enthalpies of the molecule and the corresponding cation ($IP_{g[X]} = \Delta H_{f[X^+]} - \Delta H_{f[X]}$). Because Koopman's theorem is based on the assumption of a "vertical" ionization and, therefore, does not consider the stabilization of the system due to changes in the geometry of the cation radical, the second method ("adiabatic" process) was used for further calculations. To avoid local minima pitfalls in systems with no dihedral angles, the optimization was performed at least three times using different starting structures. They were randomly generated with molecular dynamics calculations using the simulated annealing feature of HyperChem.

Results and Discussion

Ground-State Properties. The absorption spectra of aqueous PTL-HCl solution present two main bands in the UV region (Figure 1), one band with maximum absorption at 292 nm and another presenting two shoulders at 208 and 227 nm, in agreement with spectra reported by Kochevar.³ The shape and λ_{max} of these bands are solvent-independent. Similar ground-state absorption spectra were obtained for PTL. Thus, the *N*-methylpropylamino side chain protonation does not affect the ground-state electronic transitions. The quantum chemical calculations predict at least eight stable conformations for the ground state for both PTL and PTL-HCl (Table 1).

For each compound, these are all energetically very close to each other and differ only in the torsion angles of the tricyclic ring and the corresponding angle with the alkyl chain. The average torsion angle for the cyclic system in PTL-HCl is $71.0^\circ \pm 0.4^\circ$. In PTL, this angle is affected by the orientation of the alkyl chain in space. When the chain flips from the back of the suberenyl system to the front face, the molecule flattens by 17° . This effect is not observed in PTL-HCl because the bulky HCl group does not allow the chain to face the suberenyl moiety. For each compound, all corresponding stable conformations show four relatively strong transitions at the same wavelengths ± 1 nm. In PTL, they are blue-shifted by 3–15 nm relative to those of PTL-HCl. This shift effect is very small at the absorption maximum, resulting in very similar absorption spectra for both compounds. Figure 2 shows the HyperChem-calculated molecular orbitals involved in these transitions for PTL-HCl. The same orbitals participate in the case of PTL.

There are two different types of $\pi \rightarrow \pi^*$ transitions depending on the interactions of the cycloheptene double bond and the

TABLE 1: Geometrical, Thermodynamic, and Absorption Properties of the Three Lowest Energy Ground State and Excited State Most Stable Conformations of Protriptyline and Related Compounds

drug	conf	torsion angle (deg)	chain torsion angle (deg)	ΔH_f (kcal/mol)	μ (D)	λ_{max} [<i>f</i>] (nm)
PTL-HCl	$S_0(1)$	71.1	−158.6	23.0	5.1	297 [0.22], 244 [0.18], 236 [0.19], 220 [0.84]
						298 [0.22], 246 [0.19], 236 [0.17], 219 [0.81]
						298 [0.22], 246 [0.19], 236 [0.16], 218 [0.81]
	$S_0(2)$	71.3	−159.8	24.2	5.0	298 [0.22], 246 [0.19], 236 [0.17], 219 [0.81]
						298 [0.22], 246 [0.19], 236 [0.16], 218 [0.81]
						298 [0.22], 246 [0.19], 236 [0.16], 218 [0.81]
	$S_0(3)$	70.6	−149.6	24.3	4.9	298 [0.22], 246 [0.19], 236 [0.16], 218 [0.81]
						298 [0.22], 246 [0.19], 236 [0.16], 218 [0.81]
						298 [0.22], 246 [0.19], 236 [0.16], 218 [0.81]
PTL	$T_1(1)$	76.3	82.5	69.5	4.8	451 [0.05], 340 [0.03]
						451 [0.05], 340 [0.03]
						451 [0.05], 340 [0.03]
	$T_1(2)$	76.8	155.9	70.4	4.3	463 [0.05], 348 [0.03]
						463 [0.05], 348 [0.03]
						463 [0.05], 348 [0.03]
	$T_1(3)$	75.8	79.4	70.4	4.4	450 [0.05], 338 [0.02]
						450 [0.05], 338 [0.02]
						450 [0.05], 338 [0.02]
PTL	$S_0(1)$	71.2	−159.2	53.4	1.1	294 [0.32], 226 [0.51], 218 [0.70], 213 [0.53]
						294 [0.32], 226 [0.51], 218 [0.70], 213 [0.53]
						294 [0.32], 226 [0.51], 218 [0.70], 213 [0.53]
	$S_0(2)$	88.4	68.7	53.5	1.2	295 [0.31], 227 [0.50], 216 [0.61], 214 [0.56]
						295 [0.31], 227 [0.50], 216 [0.61], 214 [0.56]
						295 [0.31], 227 [0.50], 216 [0.61], 214 [0.56]
	$S_0(3)$	88.8	68.7	53.6	1.2	295 [0.31], 228 [0.50], 216 [0.61], 214 [0.56]
						295 [0.31], 228 [0.50], 216 [0.61], 214 [0.56]
						295 [0.31], 228 [0.50], 216 [0.61], 214 [0.56]
DBCH	$T_1(1)$	60.2	−79.8	99.6	1.1	455 [0.06], 355 [0.04]
						455 [0.06], 355 [0.04]
						455 [0.06], 355 [0.04]
	$T_1(2)$	65.1	−155.0	99.9	1.0	461 [0.05], 362 [0.05]
						461 [0.05], 362 [0.05]
						461 [0.05], 362 [0.05]
	$T_1(3)$	65.0	−156.0	100.0	1.1	460 [0.05], 362 [0.05]
						460 [0.05], 362 [0.05]
						460 [0.05], 362 [0.05]
DBCH	$S_0(1)$	65.7		60.5	0.08	302 [0.12], 237 [1.12], 206 [0.92]
						302 [0.12], 237 [1.12], 206 [0.92]
						302 [0.12], 237 [1.12], 206 [0.92]
DBCH	$T_1(1)$	53.0		105.8	0.3	449 [0.04], 348 [0.05]
						449 [0.04], 348 [0.05]
						449 [0.04], 348 [0.05]

benzene rings. The $\pi \rightarrow \pi^*$ hyperconjugation induces the red-shifted band at 293 nm, while the benzenoid transitions are responsible for the UVC band and, of course, for the corresponding vibronic hyperstructure. For comparison purposes, the quantum chemical calculations for the parent compound DBCH were also performed. The absence of the *N*-methylpropylamino side chain results in a decrease in the torsion angle around the C5 and the benzene rings. The DBCH cyclic system is more planar than PTL-HCl, and the corresponding electronic transitions change accordingly; the benzenoid transitions are greatly favored. The DBCH calculated UV absorption spectrum consists of two fully allowed transitions at 206 and 236 nm with oscillator strength of 0.92 and 1.12, respectively. Another transition is also predicted at 302 nm ($f = 0.12$). The agreement between the properties of DBCH and those of protriptyline provides additional support to the assigned transitions for PTL-HCl. A property significantly perturbed by the presence of the side chain is the ground-state dipole moment. The quantum theoretical calculations predict dipole moments of 5.0, 1.2, and 0.08 D for PTL-HCl, PTL, and DBCH, respectively. This difference is, obviously, explained in terms of the induced

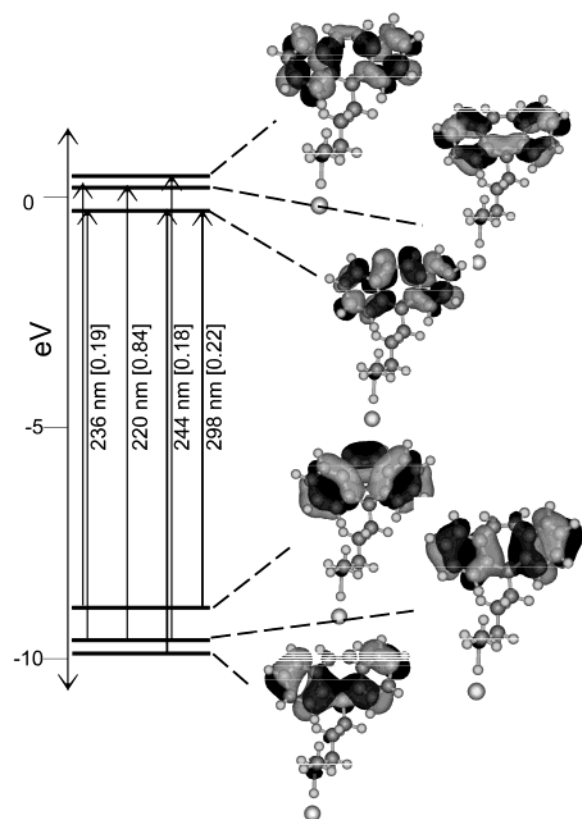


Figure 2. Molecular orbitals involved in the electronic transitions of protriptyline hydrochloride.

TABLE 2: Excited-State Photophysical Properties of PTL-HCl and PTL in Different Solvents

drug	solvent ^a	ϕ_f^b	τ_f^b (ns)	$k_f^o \times 10^8$ (s ⁻¹)	ϕ_T	τ_T (μ s)	$\phi_f + \phi_T$
PTL-HCl	PBS 7.4	0.62 (0.63)	2.56 (2.61)	2.42	0.14	96	0.76
	methanol	0.55 (0.55)	2.38 (2.09)	2.31	0.18	41	0.73
	2-propanol	0.40	1.55	2.58	0.16	75	0.56
	acetonitrile	0.56	2.41	2.32	0.15	42	0.71
PTL	methanol	0.39	2.20	1.77	0.26	34	0.65
	2-propanol	0.39	1.68	2.32	0.26	62	0.65
	acetonitrile	0.22	1.42	1.55	0.10	34	0.32
	cyclohexane	0.24	0.99	2.42	0.52	35	0.76

^a Taft's β -values are as follows: water 0.18; methanol 0.62; 2-propanol 0.95; acetonitrile 0.31; cyclohexane 0.00. ^b Values in parentheses correspond to nitrogen-saturated solutions.

polarity of the side chain. In fact, many antidepressive drugs with this side chain have been found to behave as surfactants in aqueous solutions. In this case, the *N*-methylpropylamino side chain and the dibenzocycloheptene moieties resemble the polar and nonpolar heads, respectively.

Excited Singlet-State Properties. The room-temperature PTL-HCl fluorescence spectrum consists of a broad band with maximum at 360 nm (Figure 1). An S_0 – S_1 energy difference of 88 kcal/mol was calculated from the crossing point of the excitation and emission spectra. Similar to the absorption spectrum, the emission maximum does not change with solvent. However, ϕ_f is a function of solvent. The fluorescence quantum yield of PTL-HCl is relatively high in the solvents tested (Table 2). In comparison to *cis*-stilbene, this high ϕ_f for PTL derivatives is explained in terms of the presence of the C_9 – C_{10} double bond, which increases its molecular rigidity, resulting in a decrease in the nonradiative rate constant. Similar arguments were used

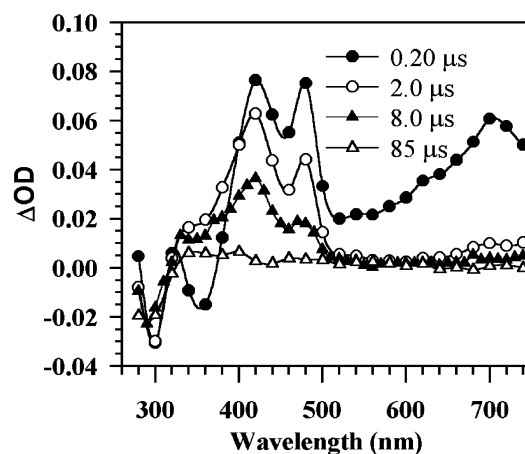


Figure 3. Transient intermediates from the 266 nm laser flash photolysis of PTL-HCl in N₂-saturated PBS 7.4 solution.

to explain the difference in ϕ_f between DBCH and *cis*-stilbene.^{9,10} Moreover, there is a relationship between the fluorescence quantum yield and the Taft's β -factor.¹⁸ For higher β , the quantum yield for PTL-HCl is lower and the corresponding value for PTL is higher. The value of β is a measure of the ability of the solvent to act as a hydrogen acceptor or electron pair donor toward the solute. Therefore, it is concluded that, when the solvent is "more basic", the contribution from the unprotonated species to the total fluorescence is higher.

Singlet fluorescence lifetimes for air-saturated PTL-HCl and its free base were monoexponential in all of the considered solvents. Frequency-domain emission decay of PTL-HCl in nitrogen-saturated phosphate saline buffer (PBS) 7.4 solution resulted in a fluorescence lifetime of 2.61 ns, similar to that measured for air-saturated solution. The fluorescence emission rate constants were obtained from the τ_f and ϕ_f values, and within the experimental error, these were similar in all of the solvents (Table 2).

Wan et al. reported that DBCH presents a monoexponential fluorescence lifetime of 4.6 ns in pure acetonitrile and 130 ps in 80% H₂O/CH₃CN (v/v).⁶ This decrease in lifetime in the presence of water was attributed to a rapid proton exchange in the excited state at the benzylic position through a carbanion intermediate with an 8π (4n) electron system. On the other hand, Johnston et al. did not observe a carbanion intermediate after 308 nm laser flash photolysis studies.⁸ A fluorescence lifetime of DBCH of 5.8 ns was reported by Watkins and Bayrakceken in 20% isopentane/methylcyclohexane at room temperature.⁹ The lifetimes for PTL-HCl and the free base determined in this work were lower than these previously reported values. This difference can be explained in terms of the increase in the torsion angle of the PTL chromophore by the *N*-methylpropylamino side chain. Besides, the side chain rotation from spatial conformation to spatial conformation induces a deactivation channel, thus resulting in lower τ_f .

Nanosecond Laser Flash Photolysis. The transient absorption spectra of laser irradiated PTL-HCl in different solvents are a function of the laser energy. In nitrogen-saturated aqueous solution at pH 7.4 and energies higher than 10 mJ, the spectra show bands with maxima at 420 and 475 and a broad band with a maximum at 720 nm (Figure 3).

The first depletion region observed at wavelengths shorter than 330 nm is due to ground-state absorption. The other depletion region at 360 nm is due to the fluorescence. Therefore, it is only observed at times shorter than 200 ns after the laser pulse. The visible absorption band with a maximum at 720 nm

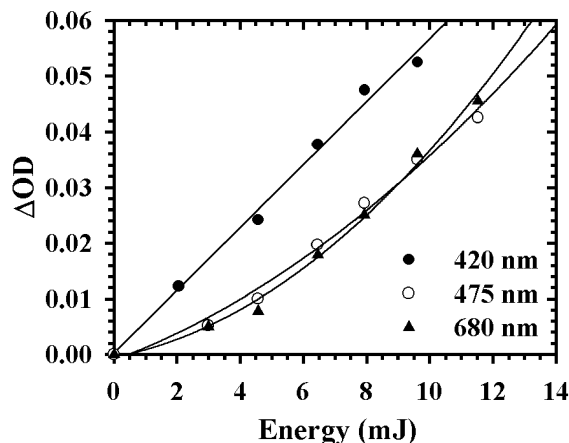


Figure 4. Photonicity of the triplet (420 nm), cation radical (475 nm), and solvated electron (680 nm) generated by 266 nm laser flash photolysis of nitrogen-saturated PTL-HCl solution in PBS 7.4 ($A_{266\text{nm}} = 0.8$). The signal at 475 nm was measured under N_2O and 0.05 M *tert*-butyl alcohol.

presents contributions from two species with different lifetimes, a short lifetime species with $\tau < 1 \mu\text{s}$ and a longer-lived one with $\tau > 3 \mu\text{s}$. The transient absorption spectrum of nitrogen-saturated cyclohexane PTL solutions with laser energies lower than 3 mJ shows only the 420 nm band ($\tau > 10 \mu\text{s}$) and the ground-state depletion. Similar results were obtained for PTL-HCl in acetonitrile and methanol solutions under low and high laser energies, although the electron absorption was not observed in these solvents.

Characterization of Triplet State. The 420 nm band was quenched by oxygen ($\tau < 0.2 \mu\text{s}$), but its intensity was not affected by the presence of N_2O . On the basis of the effects of these additives and photosensitization experiments (see below), this band was assigned to a triplet-triplet absorption of PTL-HCl. The absorbance of the 420 nm transient shows a linear dependence with laser energy as determined from the zero intercept and the corresponding slope of a log-log plot (See Figure 4; slope = 1.1). Triplet lifetimes in the different solvents were calculated from the analysis of the decay curves at 420 nm at low laser energies (Table 2). Similar results were obtained for the PTL free base.

Determination of Triplet-Triplet Molar Absorption Coefficient (ϵ_T) and Quantum Yield of Triplet Formation (ϕ_{isc}). Figure 5 depicts the transient spectra of a 355 nm irradiated 1.6 mM BP and 0.8 mM PTL-HCl acetonitrile solution. At observation times close to the end of the laser pulse, a transient absorption appears at 520 nm, which corresponds to the BP triplet state. This species decays with a lifetime of 195 ns. As the $^3\text{BP}^*$ decays, a new band is observed with maximum at 420 nm ($\tau_{\text{growth}} = 169 \text{ ns}$). These results indicate that the $^3\text{BP}^*$ sensitizes PTL-HCl through an energy transfer process.¹⁹ After the consumption of $^3\text{BP}^*$, the 420 nm band then decayed with a lifetime of 46 μs , similar to the lifetime of the PTL-HCl triplet state determined by direct excitation at low laser energy in acetonitrile. It is important to mention that, after the decay of the $^3\text{BP}^*$, there was no evidence of an electron-transfer reaction because neither the BP ketyl radical nor the PTL-HCl radical cation transient absorptions were observed. Triplet-state molar absorption coefficients of 16 000 and 12 000 $\text{M}^{-1} \text{cm}^{-1}$ were obtained for PTL-HCl and PTL from these energy-transfer experiments. The triplet-state yield of PTL-HCl was found to be almost independent of solvent with values in the range of 0.14–0.18 (Table 2). In general, ϕ_T has higher values for the free base in protic solvents than in polar aprotic ones. Interest-

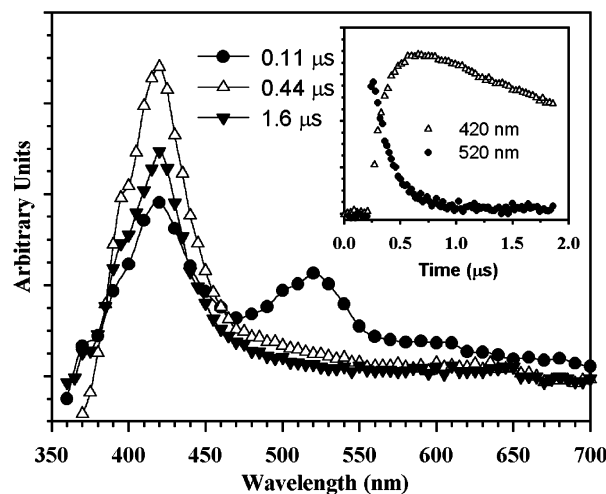


Figure 5. Triplet-triplet energy transfer from benzophenone (1.6 mM) to PTL-HCl (0.8 mM) with laser excitation at 355 nm in acetonitrile under nitrogen. The inset shows the corresponding kinetic traces.

ingly, when comparing PTL-HCl with the free base, it is observed that a decrease in the fluorescence quantum yield is accompanied by an increase in the triplet quantum yield for all solvents, except acetonitrile. For these other solvents, the decrease in the fluorescence efficiency obviously leads to an increase in the intersystem-crossing rate constant. This is observed in the fact that the total quantum yield remains almost constant ($\phi_f + \phi_T = 0.69 \pm 0.07$). In acetonitrile, on the other hand, the difference in the fluorescence quantum yield between PTL-HCl and the free base suggests a quenching effect by the protonated *N*-methylpropylamino side chain because there is no change in ϕ_T , that is, the total quantum yield actually decreases from 0.71 to 0.32. If this is the case, it must be an intermolecular effect because the side chain is more than 6 Å apart from the ring system, as obtained with PM3 calculations. This type of second-order process, nevertheless, always requires either a relative high concentration of the quenching partners or ground-state complex aggregates. Because our experiments were performed with low PTL concentrations, further characterization of this quenching effect is currently under study.

A triplet energy of approximately 66 kcal/mol had been reported for the DBCH triplet state on the basis of phosphorescence spectra.^{8,9} However, Ikeyama et al. reported a triplet-state energy of only 53 kcal/mol, also determined from the phosphorescence spectra.¹⁰ The photosensitization experiments presented in this work correlate better with a PTL triplet energy of 53 kcal/mol because the $^3\text{BP}^*$ sensitizer has an energy of 69 kcal/mol.¹⁹ An energy difference of 16 kcal/mol favors a large bimolecular rate constant (6.4×10^9 and $7.1 \times 10^9 \text{ M}^{-1} \text{s}^{-1}$ for the reaction between $^3\text{BP}^*$ and PTL-HCl and PTL, respectively). These bimolecular rate constants are close to one-third of the diffusion-controlled rate constant in acetonitrile ($2 \times 10^{10} \text{ M}^{-1} \text{s}^{-1}$).¹⁹ UHF semiempirical quantum chemical calculations are in good agreement with these predictions (Table 3).

A triplet energy for DBCH, PTL, and PTL-HCl of approximately $46 \pm 4 \text{ kcal/mol}$ was calculated, indicating that the triplet-state properties are determined by the parent moiety. This, in turn, was also corroborated by the fact that the orbitals of the T_1 state correspond to the DBCH moiety and the corresponding properties are almost constant, as illustrated by the small changes in the ionization potentials given in Table 4.

The open-shell semiempirical structure optimization predicts up to five energetically very close conformations for the triplet

TABLE 3: Excited-State Properties of the Most Stable Conformations of PTL and PTL-HCl and of Their Parent Compound DBCH Determined with Quantum Chemical Calculations

molecule	torsion angle (deg)		ΔH_f (kcal/mol)			E_T (kcal/mol)	
	S ₀	T ₁	S ₀	T ₁	cation	PM3	expt
BP	63.4	23.5	17.0	91.5		75	69
DBCH	65.7	53.0	60.5	105.8	251.1	45	53
PTL	71.1	65.0	53.4	99.6	245.4	46	
PTL-HCl	71.3	75.8	23.0	69.5	218.0	47	

state of protriptyline (Table 1), with a trans conformation in the cyclic double bond. The highest-energy binding orbital of this state has the biggest contribution from the C₉–C₁₀ double bond for DBCH and both protriptyline derivatives. The parent compound and the PTL free form have a smaller torsion angle in the triplet excited state than in the ground state, but PTL-HCl has a bigger torsion angle in the T₁ state. A triplet–triplet absorption band is predicted at 449 ± 5 nm with a relative low molar absorption extinction coefficient. The large difference between this prediction and the experimental T–T absorption maximum of 420 nm is due to the solvent effect, because almost no spin contamination was observed in our theoretical calculations.

Characterization of Radical Cations. The short-lived species absorbing in the visible region was quenched by O₂ and N₂O and at pH = 2.0. All of these additives are efficient electron scavengers, thus this species was assigned to the solvated electron. The solvated electron decay decreases linearly with PTL-HCl ground-state concentration. From a plot of the pseudo-first-order rate constant of the electron decay against the PTL-HCl concentration, a bimolecular rate constant of 1.1 × 10¹⁰ M⁻¹ s⁻¹ was calculated for the electron addition to PTL-HCl ground state. The formation of the hydrated electron is accompanied by the formation of a geminate radical cation. The shape and intensity of the band with maximum at 475 nm and the long-lived component in the visible region were not affected by the presence of oxygen or N₂O or the pH. These results indicate that this band can be assigned to the PTL-HCl radical cation. In addition, in air-saturated aqueous solution and with laser energies higher than 10 mJ, a band at 420 nm was also observed at times longer than 3 μs (Figure 6). At these times, the triplet state has already decayed, because under low laser energy its lifetime is shorter than 0.3 μs (see above). Furthermore, the decay traces recorded at 420, 475, and 780 nm (in PBS 7.4) after the complete decay of the solvated electron gave similar lifetimes under high laser energy and air-saturated conditions (3 μs). These results are very similar to those reported by Johnston et al. for DBCH and its OH derivative in acetonitrile and acetonitrile/water mixture.⁸ These authors also identified this transient intermediate as the radical cation. Thus, the *N*-methylpropylamino side chain substitution in DBCH does not seem to affect the processes leading to the formation of the transient intermediates, because similar species are observed in both cases.

The effects of the laser intensity on the radical cation and solvated electron formation were further examined. Plots of signal intensity at the end of the laser pulse at 475 and 680 nm against laser energy showed an upward curvature at high laser doses (Figure 4). These results are typical of a two-photon photoionization mechanism, as demonstrated by the nonzero intercept and slopes of 1.8 and 1.9 for the log–log plots of the data recorded at 475 and 680 nm, respectively. Although at 680 nm the solvated electron and radical cation absorb, the absorbance at the end of the laser pulse is mainly due to the former.

Similar results were observed for DBCH and the OH-derivative.⁸

The ionization potential for all compounds in solution (IP_{solution}) was determined using the following equation:²⁰

$$\text{IP}_{\text{solution}} = \text{IP}_{\text{g}} + P_{+} + V_0 \quad (4)$$

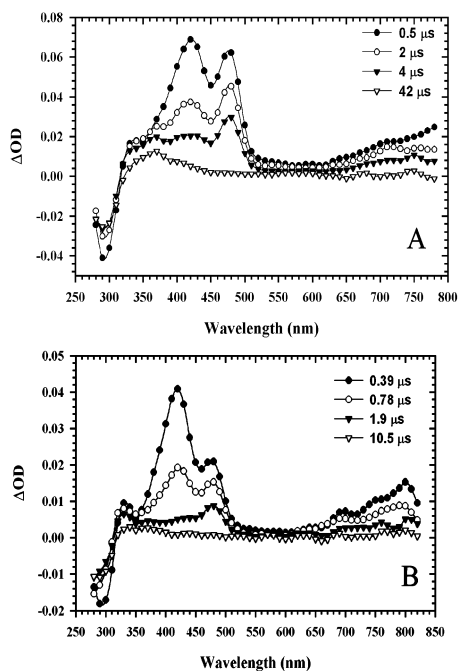
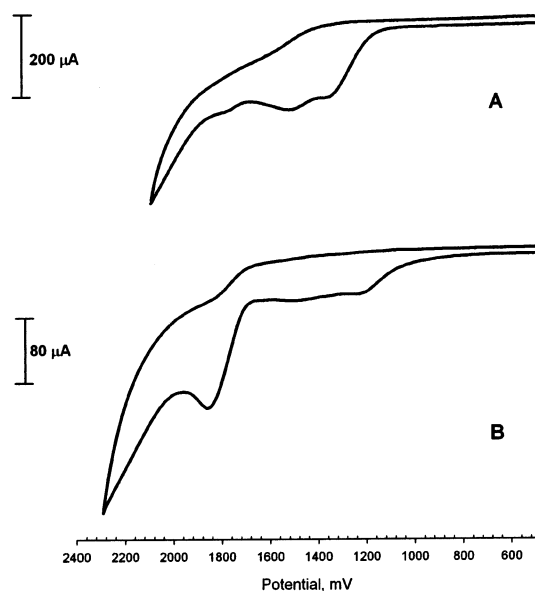
In this equation, IP_g is the ionization potential in the gas phase, P_{+} is the adiabatic electronic polarization energy of the medium by the positive ion, and V_0 is the ground-state energy of the “quasi-free” electron in the liquid relative to the electron in a vacuum. The IP_g values were determined from the difference in formation enthalpies, as described in the Experimental Section. The value of P_{+} was obtained using Born’s equation: $P_{+} = -e'(\epsilon - 1)/(2r^{+}\epsilon)$, where $e' = e^2/(4\pi\epsilon_0)$, ϵ is the solvent optical dielectric constant, and r^{+} is the cation radius (calculated from the molecular volume, which is obtained using the grid method implemented in HyperChem). V_0 has the following values: −1.5 eV for acetonitrile,^{21,22} −1.3 eV for water, and −1.0 eV for methanol.²² All other calculated values are summarized in Table 4, including Koopman’s ionization potentials. As mentioned before, the relatively higher values of this quantity are attributed to the stabilization of the cation radical. IP_{solution} values bigger than 5.6 eV were estimated for PTL and PTL-HCl in both solvents. Because this IP_{solution} value is larger than the 266 nm laser photon energy (4.7 eV), the molecule must absorb two photons to produce states with energies exceeding 9.4 eV. The nature of the excited state leading to photoionization is still unclear, because in two-color experiments with the DBCH alcohol derivative, the second laser pulse did not bleach the triplet transient and the transient band of the radical cation production was not observed.⁸ This suggested, according to the authors, that re-excitation of the triplet was not responsible for the radical cation formation. Therefore, the S₁ state, with a lifetime of 2–5 ns, was proposed as the state absorbing the second photon during the nanosecond laser pulse. This time is long enough for the S₁ to absorb a second photon within the laser pulse. Similar behavior can be expected for PTL-HCl and its free base.

Figure 7 shows the cyclic voltammograms of 3 mM PTL-HCl and PTL solutions in acetonitrile. Both compounds show an oxidation peak at 1.78 V (PTL-HCl) and 1.85 V (PTL) vs Ag/AgCl(sat). A shoulder is observed for PTL-HCl at 1.52 V. The two oxidation peaks for both PTL-HCl and its free base are attributed to short-lived intermediates, which are not sufficiently stable to generate the corresponding reduction peaks within the time of the experiment (10 s). Small distortions observed in all voltammograms are produced by the adsorption of the species on the electrodes, as corroborated with the scan-rate variations. These experimental oxidation potentials indicate that the free base has a relatively lower oxidation ability than PTL-HCl. The oxidation potentials obtained for PTL-HCl and its free base are higher than the oxidation peak potential of the parent hydrocarbon DBCH in acetonitrile ($E = 1.59$ V).⁸ This indicates that the 5-substituent in PTL-HCl and its free base decreases the ability of the radical cation to form. The peaks are assigned to the cation radical formation, as proposed for other substituted dibenzosuberonyl systems.⁸ UHF-PM3 calculations show that the spin density shifts from C₉–C₁₀ to C₅ after the deprotonation of the cation radical. C₅ had previously been proposed as the deprotonation center in DBCH, because it stabilizes the neutral radical. This is why DBCH has been proposed as intermediate for organic synthesis. In the case of PTL-HCl, the formation of this C₅-centered radical is even more probable, because it increases the conjugation of the ring system

TABLE 4: Ionization and Oxidation Potentials of PTL, PTL-HCl, and DBCH in Methanol ($\epsilon = 32.6$ D) and Acetonitrile ($\epsilon = 37.5$ D)

molecule	$V(\text{\AA}^3)$	$\text{IP}_{\text{gas}} (\text{eV})$		$\text{IP}_+ (\text{eV})$		$\text{IP}_{\text{solution}} (\text{eV})^c$		ox potential (V)	
		<i>a</i>	<i>b</i>	CH_3OH	CH_3CN	CH_3OH	CH_3CN	CH_3OH	CH_3CN
DBCH	624.8	8.8	8.3	1.32	1.32	5.95	5.44		1.59 ^d
PTL	855.8	8.9	8.3	1.19	1.19	6.14	5.63	1.63	1.85
PTL-HCl	932.5	9.0	8.3	1.15	1.16	6.17	5.67	1.56	1.78

^a Obtained from Koopman's theorem. ^b Calculated with the formation enthalpy of the molecule and the corresponding cation. ^c Calculated with the "adiabatic" gas ionization potential. ^d Reference 8.

**Figure 6.** Transient absorption spectra of PTL-HCl at high laser energy (A) in air-saturated PBS 7.4 solution and (B) in nitrogen-saturated methanol solution.**Figure 7.** Cyclic voltammograms of 3 mM solutions of (A) PTL-HCl and (B) PTL free base in 0.1 M tetrabutylammonium perchlorate in acetonitrile. The working electrode is glassy carbon, the reference electrode is Ag/AgCl(sat), and the counter electrode is Pt.

and it is a tertiary carbon. The reactivity of this neutral radical explains why the oxidation process is an irreversible process.

Quantum Yields of $^1\text{O}_2$ Formation, $\phi(^1\text{O}_2)$. The participa-

tion of the singlet oxygen in the photochemistry of PTL-HCl was established by measuring the RNO bleaching according to Kochevar and Redmond.¹⁷ PTL-HCl promotes singlet oxygen formation as evidenced by the observed RNO bleaching. To determine whether RNO bleaching occurred only through triplet energy transfer, a system without imidazole was subjected to the same steady-state photolysis conditions. Only a small decrease in the slope for the system without imidazole was observed, indicating that the major RNO bleaching occurs through energy transfer. Furthermore, photolysis of a solution without PTL-HCl did not result in bleaching of RNO. To corroborate the exclusive role of singlet oxygen as the RNO bleaching agent, the reactivity of singlet oxygen was examined in the presence of 1.0 mM azide. Under these conditions, singlet oxygen was expected to be effectively scavenged by the azide ion ($k_q = 2.8 \times 10^8 \text{ M}^{-1} \text{ s}^{-1}$).^{15,16} The results show that azide decreases the RNO bleaching, although complete RNO bleaching inhibition was not observed under those conditions. These results suggest that, under our conditions, the RNO bleaching occurs not only through energy transfer but also through a radical mechanism. Probably the radical mechanism is initiated by a reaction between PTL-HCl and the azide ion. In fact, the PTL-HCl triplet state was quenched by the azide ion with a bimolecular rate of $6.3 \times 10^5 \text{ M}^{-1} \text{ s}^{-1}$, as determined by 266 nm laser flash photolysis and Stern–Volmer analysis. Nevertheless, the interaction between the PTL triplet state and oxygen is clearly demonstrated by these results. To calculate the PTL-HCl singlet oxygen quantum yield, the difference of slopes under steady-state irradiation conditions with and without imidazole was determined and substituted in eq 3. This difference corresponds to only the energy-transfer process. Using this value and the corresponding slope for PH and its singlet oxygen quantum value of 1.0, we calculated the PTL-HCl singlet oxygen quantum in PBS 7.4 to be 0.06. In principle, the singlet oxygen formation can have contributions from the excited singlet and the triplet states. Because the PTL-HCl excited singlet state was not quenched by oxygen (see above), all of the singlet oxygen must be produced from the PTL-HCl triplet state. Therefore, a triplet quenching efficiency value (S_Δ) of 0.43 was determined.

Conclusion

The photochemical behavior of PTL-HCl in the presence and absence of oxygen had been previously studied by Kochevar and Gasparro.² They found that, in the presence of oxygen, irradiated PTL-HCl solutions turned yellow and turbid because of the formation of a mixture of photoproducts. Under anaerobic conditions, however, the solution remained clear and HPLC and MS analysis showed the presence of only two new photoproducts. One of these photoproducts was identified as the PTL-HCl cyclobutyl dimer. In related studies, Jones and Sharples isolated three PTL-HCl photoproducts under oxygen and identified these as the 10,11-epoxide, 10-hydroxy, and 10,11-dihydrodiol PTL-HCl derivatives.⁴ Both studies present data that strongly suggest the participation of the PTL-HCl triplet state

in its photochemistry. This state has been fully characterized in the present work. The PTL-HCl triplet state was populated by absorption of UV light in almost 15% yield and presents lifetimes in the microsecond range in the studied solvents. The properties of the triplet state presented in this work support its involvement in the PTL-HCl cyclobutyl dimer mechanism at low irradiation intensity. This is sustained by the fact that, under aerobic conditions, no dimer is produced. However, dimer formation is due to the cycloheptene double-bond reactivity and requires high analytical drug concentrations. The double-bond reactivity could be enhanced in cellular membranes, because it is known that the tricyclic antidepressive drugs have high affinity for hydrophobic environments. Previous reports established that epoxidation of the corresponding ethylenic linkage was found to be a common pathway of 5*H*-dibenzo[*a,d*]cycloheptene, iminostilbene, and *trans*- and *cis*-stilbene. Interestingly, these epoxides were further oxidized to dihydrodiols and α -hydroketones. Moreover, these authors reported that the radical scavenger 2,6-bis(1,1-dimethylethyl)-4-methylphenol (BHT) decreases the total conversion yield. Under direct excitation of DBCH, radicals may be produced from its triplet state under oxidative conditions.^{24,25} According to our data, oxygen quenches the PTL-HCl triplet state with a bimolecular rate constant in the range of $(4.37\text{--}7.54) \times 10^8 \text{ M}^{-1} \text{ s}^{-1}$. Obviously, this explains why there is no dimer formation. Nevertheless, the epoxide, hydroxy, and dihydrodiol derivatives identified by Jones and Sharples can be produced through an oxygen-triplet reaction.⁴ The PTL-HCl triplet can produce singlet oxygen and superoxide radical by energy or electron transfer, respectively. Therefore, type I and type II photochemistry could lead to the corresponding PTL-HCl oxygenated products. Singlet oxygen is known to be very reactive toward alkenes. Also, the superoxide radical could disproportionate in water leading to a hydroxy radical, which can add to alkenes yielding the hydroxy products. In conclusion, the PTL-HCl triplet state is involved in the dimer formation and other reactive intermediates. Therefore, it is the most probable species to be responsible for the phototoxic effects observed for this drug.

Acknowledgment. This work has been supported in part by NIH-MBRS Grant S06GM08216. R. Oyola also appreciates

the financial support from GAAN fellowship program and the Puerto Rico Industrial Development Company.

References and Notes

- (1) Kochevar, I. E. *Toxicol. Appl. Pharmacol.* **1980**, *54*, 258.
- (2) Kochevar, I. E.; Gasparro, F. *Photochem. Photobiol.* **1982**, *35*, 351.
- (3) Kochevar, I. E.; Lamola, A. A. *Photochem. Photobiol.* **1979**, *29*, 791.
- (4) Jones, G. E.; Sharples, D. J. *Pharm. Pharmacol.* **1984**, *36*, 46.
- (5) Wan, P.; Krogh, E.; Chak, B. J. *Am. Chem. Soc.* **1988**, *110*, 4073.
- (6) Wan, P.; Budac, D.; Earle, M.; Shukla, D. J. *Am. Chem. Soc.* **1990**, *112*, 8048.
- (7) Johnston, L.; Azarani, A.; Berinstein, A. B.; Kazanis, S. J. *Photochem. Photobiol. A: Chem.* **1991**, *57*, 175.
- (8) Johnston, L.; Lobaugh, J.; Wintgens, V. J. *Phys. Chem.* **1989**, *93*, 7370.
- (9) Watkins, A. R.; Bayrakceken, F. J. *Luminesc.* **1980**, *21*, 239.
- (10) Ikeyama, T.; Kabuto, C.; Dato, M. J. *Phys. Chem.* **1996**, *100*, 19289.
- (11) Lakowicz, J. *Principles of fluorescence spectroscopy*; Plenum Press: New York, 1999.
- (12) Demas, J.; Crosby, G. J. *Phys. Chem.* **1971**, *75*, 991.
- (13) Beck, G. *Rev. Sci. Instrum.* **1976**, *47*, 537.
- (14) Bensasson, R. V.; Land, E. J.; Truscott, T. G. *Excited states and free radicals in biology and medicine: contributions from flash photolysis and pulse radiolysis*; Oxford University Press: New York, 1993; Chapter 5.
- (15) Kraljic, I.; Mohsni, E. *Photochem. Photobiol.* **1978**, *28*, 577.
- (16) Kraljic, L.; Verlhac, J. B.; Gaudemer, A. *Nouv. J. Chim.* **1984**, *8*, 401.
- (17) Kochevar, I. E.; Redmond, R. W. Photosensitized production of singlet oxygen. In *Singlet Oxygen, UV-A and Ozone*; Packer, L., Sies, H., Eds.; Methods in Enzymology, Vol. 319; Academic Press: San Diego, CA, 2000; p 20.
- (18) Kamelt, M.; Abboud, J. L.; Abrahm, M.; Taft, R. W. *J. Org. Chem.* **1983**, *48*, 2877.
- (19) Turro, N. J. *Modern molecular photochemistry*; University Science Book: Sausalito, CA, 1991.
- (20) Ogawa, T.; Ogawa, T. *J. Phys. Chem. A* **1998**, *102*, 10608.
- (21) Murgida, D. H.; Bilmes, G. M.; Erra-Balsells, R. *Photochem. Photobiol.* **1996**, *64*, 777.
- (22) Faria, J. L.; Steenken, S. J. *Phys. Chem.* **1993**, *97*, 1924.
- (23) Amouyal, E.; Bernas, A.; Grant, D. *Faraday Discuss. Chem. Soc.* **1982**, *74*, 147.
- (24) Zbaida, S.; Kariv, R. *Biopharm. Drug Dispos.* **1990**, *11*, 39.
- (25) Pantaroto, C.; Cappellini, L.; Frigerio, A. *J. Chromatogr.* **1977**, *131*, 430.